T-cadherin is critical for adiponectin-mediated cardioprotection in mice

Martin S. Denzel,[1] Maria-Cecilia Scimia,[1,2] Philine M. Zumstein,[1] Kenneth Walsh,[3] Pilar Ruiz-Lozano,[1] and Barbara Ranscht[1]

[1]Sanford-Burnham Medical Research Institute, La Jolla, California, USA. [2]Department of Medicine, University of California San Diego, La Jolla, California, USA. [3]Molecular Cardiology/CVI, Boston University School of Medicine, Boston, Massachusetts, USA.

The circulating, adipocyte-secreted hormone adiponectin (APN) exerts protective effects on the heart under stress conditions. The receptors binding APN to cardiac tissue, however, have remained elusive. Here, we report that the glycosyl phosphatidylinositol–anchored cell surface glycoprotein T-cadherin (encoded by *Cdh13*) protects against cardiac stress through its association with APN in mice. We observed extensive colocalization of T-cadherin and APN on cardiomyocytes in vivo. In T-cadherin–deficient mice, APN failed to associate with cardiac tissue, and its levels dramatically increased in the circulation. Pressure overload stress resulted in exacerbated cardiac hypertrophy in T-cadherin–null mice and paralleled corresponding defects in mice lacking APN. During ischemia-reperfusion injury, the absence of T-cadherin increased infarct size similar to that in APN-null mice. Myocardial AMPK is a major downstream protective signaling target of APN. In both cardiac hypertrophy and ischemia-reperfusion models, T-cadherin was necessary for APN-dependent AMPK phosphorylation. In APN-null mice, recombinant adenovirus-expressed APN reduced exaggerated hypertrophy and infarct size and restored AMPK phosphorylation as previously reported. In contrast, rescue was ineffective in mice lacking T-cadherin in addition to APN. These data suggest that T-cadherin protects from stress-induced pathological cardiac remodeling by binding APN and activating its cardioprotective functions.

Introduction

Acute or chronic stress to the heart leads to pathological remodeling that can result in heart failure. Acute myocardial ischemia is caused by insufficient coronary blood supply of the myocardium through reduced afferent flow. Rapid reperfusion therapy, such as thrombolysis or percutaneous intervention, is able to reduce mortality by restoring blood flow to the ischemic area. Such treatment, however, often leads to reperfusion injury characterized by irreversible cell damage, including necrosis and apoptosis (1). Chronic stress caused by pressure overload induces cardiac hypertrophy to preserve contractility (2). While early responsive cardiomyocyte growth is compensatory, prolonged pressure or volume overload predisposes to congestive heart failure through ventricular wall thinning and chamber dilation (3).

Heart disease is the major cause of death in Western countries (4, 5). Therefore, mechanisms that enhance cardioprotective pathways while counteracting damage are of great clinical interest. A major etiological risk factor for heart disease is the metabolic syndrome, defined as the concurrence of dysregulated glucose and insulin metabolism, increased BMI (>25), abdominal fat deposition, hyperlipidemia, and hypertension. Adiponectin (APN; also referred to as ACRP30 or AdipoQ) is an adipocyte-derived hormone with beneficial metabolic and cardiovascular properties. APN levels in the circulation of lean healthy individuals range between 5 and 30 μg/ml and decrease in persons with metabolic syndrome (6, 7). Numerous clinical and epidemiological studies correlate low APN serum levels with development of coronary artery disease, myocardial infarction, hypertension, LV hypertrophy, and other cardiovascular dysfunctions (8–12).

While much is known about the dysregulation of APN in various diseases, the mode by which APN associates with target tissues and exerts physiological effects is poorly understood. Expression cloning approaches identified 3 candidate plasma membrane APN receptors. AdipoR1 and AdipoR2 are 7-span transmembrane APN receptors with structural differences from G protein–coupled receptors, such as an inverse membrane topology (13). Both receptors are ubiquitously expressed, with tissue-specific levels varying between subtypes (13). Studies with KO mice implicate AdipoR1 and -R2 in liver and muscle-dependent regulation of glucose and lipid metabolism, although independent receptor KO strains produce diverging results for the respective roles of AdipoR1 and -R2 in metabolic function (14–17). The roles of AdipoR1 and -R2 remain obscure in the heart.

T-cadherin (encoded by *Cdh13*) was identified as an APN receptor by its ability to specifically bind the physiological high–molecular weight (HMW) APN isoforms in vitro (18). This cadherin family cell surface glycoprotein shares the ectodomain structure of classical cadherins but differs in its plasma membrane anchor through a glycosyl phosphatidylinositol moiety (19, 20). We previously demonstrated that T-cadherin promotes calcium-dependent, homotypic cell-cell adhesion that serves to regulate the fine-tuned pattern of axon projections in the developing vertebrate nervous system (21–23). Critical residues in extracellular domain 1 generate a novel X-dimer cadherin-binding interface to mediate this function (24). We and others noted abundant T-cadherin expression in the myocardium and reported T-cadherin's association with cholesterol-rich membrane domains (known as lipid rafts) of the cardiac sarcolemma (25). This profile, together with genetic linkage studies associating mutations in the human *Cdh13* gene with APN serum concentrations (26) and metabolic diseases including obesity, hyperlipidemia (26), blood pressure dysregulation (27), and LV wall thickness (28), raised our interest in investigating T-cadherin functions in the heart.

We generated T-cadherin–null (Tcad-KO) mutant mice, which live well into adulthood without overt pathological phenotypes (29). Challenging these animals in a mouse mammary tumor

Conflict of interest: The authors have declared that no conflict of interest exists.
Citation for this article: *J Clin Invest.* 2010;120(12):4342–4352. doi:10.1172/JCI43464.

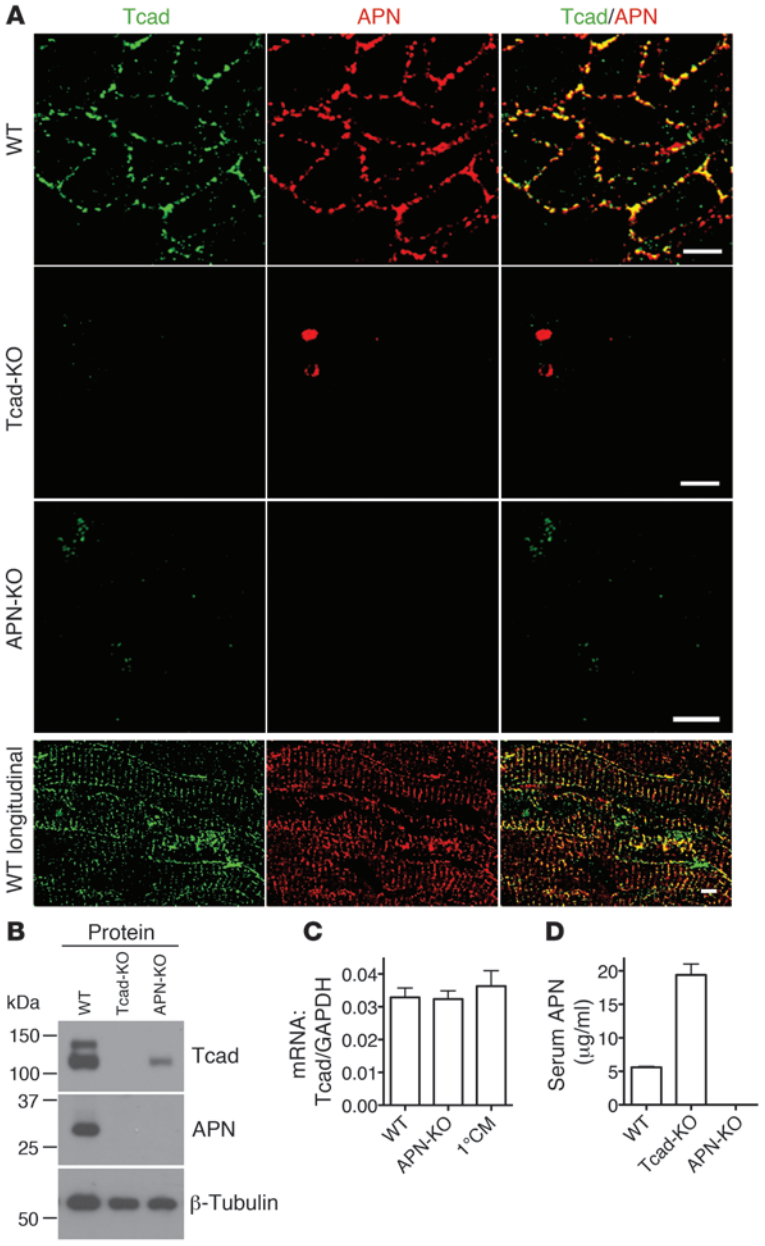

Figure 1
T-cadherin and APN in the heart. (**A**) Immunostaining of WT, Tcad-KO, and APN-KO hearts using T-cadherin and APN antibodies. Scale bars: 5 μm. (**B**) Immunoblot of myocardial lysates of the indicated genotypes. T-cadherin was detected as a doublet in the 130-kDa pro-protein and the proteolytically cleaved 105-kDa mature isoforms. Denatured APN appeared as a single 30-kDa band. (**C**) Expression levels of T-cadherin mRNA in the myocardium of WT and APN-KO mice and in isolated cardiomyocytes (1°CM). (**D**) Serum APN ELISA from WT, Tcad-KO, and APN-KO mice. $P < 0.0001$, WT versus Tcad-KO.

model uncovered a proangiogenic role for T-cadherin in tumor vascularization (29). Here, we used these Tcad-KO mice to investigate T-cadherin's physiological functions in the heart. Our results showed that T-cadherin is critically required for the association of APN with the myocardium. Importantly, ablation of T-cadherin abolished APN's cardioprotective effects in short- and long-term cardiac hypertrophy as well as in myocardial ischemia-reperfusion injury and disrupted the activation of a major APN signaling pathway converging on AMPK. These data suggest that T-cadherin binds APN and is necessary for APN-mediated cardioprotection.

Results

T-cadherin is required to sequester APN to the heart. We first established the localization of T-cadherin in the myocardium in adult WT mice. T-cadherin immunohistochemistry resolved discrete puncta on the surfaces of cross-sectioned cardiomyocytes, consistent with T-cadherin's lipid raft association (25). APN staining prominently overlapped with the T-cadherin pattern in cross-sections and on the sarcolemma in longitudinal views of cardiomyocytes (Figure 1A). To test whether T-cadherin plays an active role in sequestering APN, we investigated APN distribution in the hearts of Tcad-KO mice. In Tcad-KO hearts, APN association with cardiomyocytes was undetectable, with staining reduced to background levels (Figure 1A). Conversely, investigation of APN-KO hearts for T-cadherin expression revealed obvious downregulation of the T-cadherin signal.

Western blotting of heart lysates further supported the interrelation between T-cadherin and APN (Figure 1B). Both T-cadherin and APN were abundant in WT myocardium. Consistent with the immunostaining results, APN was not detected in Tcad-KO heart tissue, and T-cadherin protein expression was markedly reduced in the APN-KO myocardium (Figure 1B). The reduction of T-cadherin protein in APN-KO hearts occurred at the posttranscriptional level, as mRNA levels were comparable in WT and APN-KO mice (Figure 1C). Moreover, quantitative PCR (qPCR) showed that T-cadherin mRNA was expressed in isolated cardiomyocytes (Figure 1C). AdipoR1 and -R2 have been shown to mediate APN signaling in skeletal muscle and liver (13, 15), and are thus generally thought to perform similar functions in the heart. By testing protein and mRNA abundance in the heart, we found that AdipoR1 and -R2 were expressed in the myocardium, and levels were independent of the genotype of the mutant mice used in this study (Supplemental Figure 1; supplemental material available online with this article; doi:10.1172/JCI43464DS1). ELISA measurements of APN in serum revealed a significant increase, from an average concentration of 5.6 μg/ml in WT to 19.4 μg/ml in Tcad-KO mice (Figure 1D). This marked increase in circulating APN levels combined with loss of tissue-bound APN in Tcad-KO mice is consistent with the suggestion that T-cadherin sequesters APN to the heart.

T-cadherin directly interacts with APN. We next aimed to test whether the interaction between T-cadherin and APN is direct. We incubated differentiated C2C12 myotubes expressing endogenous T-cadherin with HMW APN and used specific antibodies to immunoprecipitate APN from cell lysates following cross-linking. Indeed, T-cadherin was coimmunoprecipitated in a complex with APN (Figure 2A), which suggests a direct biochemical interaction. Moreover, transfection of T-cadherin into HEK293 cells was sufficient to bind mouse serum APN to the cultured cells. In

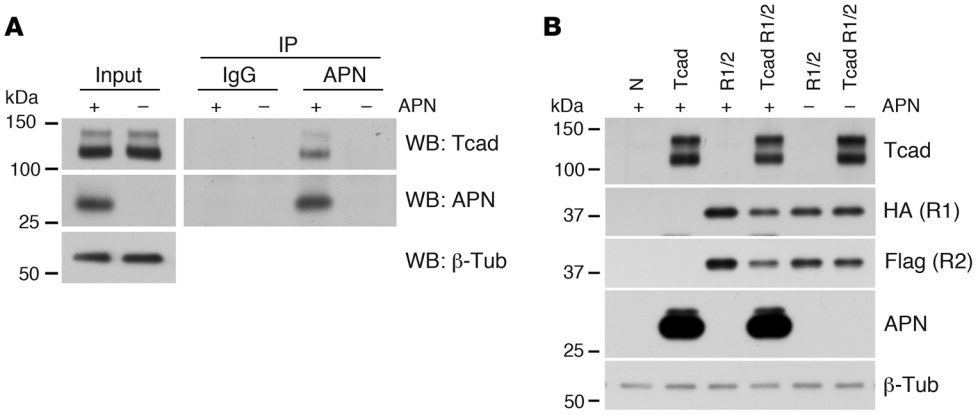

Figure 2

T-cadherin directly binds APN. (**A**) Differentiated C2C12 myotubes were treated with 25 μg/ml HMW APN for 30 minutes, washed with PBS, and cross-linked with dimethyl 3,3′-dithiopropionimidate dihydrochloride. Lysates were subjected to immunoprecipitation with unspecific IgGs or APN antibodies. (**B**) HEK293 cells stably transfected with pL-N1 control (N) or pL–T-cadherin were transiently transfected with HA-AdipoR1 or Flag-AdipoR2 coding constructs using the calcium phosphate method. Cells were incubated with 1:10 diluted serum from Tcad-KO (+ APN) or DKO mice (– APN) and subsequently washed 3 times with PBS. Immunoblotting using the indicated antibodies revealed presence of the respective proteins; AdipoR1 and -R2 were detected using the respective tags.

contrast, and consistent with our in vivo observations, association of APN was undetectable when AdipoR1 and -R2 were ectopically expressed in HEK293 cells in the absence of T-cadherin (Figure 2B). While these basic observations do not exclude the utility of AdipoR1 or -R2 in mediating APN-induced signal transduction events in the heart, our data suggested that T-cadherin is required for sequestering physiological APN isoforms to their site of action. Therefore, we next tested the hypothesis that T-cadherin is a critical mediator of cardiac APN function.

Tcad-KO mice display exaggerated hypertrophy 7 days after TAC. The strong codependence of cardiac T-cadherin expression and APN association raised the possibility that loss of T-cadherin renders the myocardium insensitive to APN's cardioprotective activity. To test this model, we analyzed cardiac hypertrophy during transaortic constriction–induced (TAC-induced) pressure overload in Tcad-KO mice. The pressure overload–induced hypertrophic phenotype has previously been established for APN-KO mice (30, 31). For reference, we therefore carried out all experiments in parallel with APN-KO mice. WT mice served as negative controls.

Hearts from Tcad-KO and APN-KO mice displayed no overt abnormalities under baseline conditions (data not shown). Consistent with this, hearts of sham-operated WT, Tcad-KO, and APN-KO mice were also similar in size (Figure 3A). TAC, as expected, resulted in compensatory hypertrophy in WT hearts 7 days after surgery and markedly exaggerated concentric hypertrophy in the APN-KO condition (Figure 3A), as previously reported (31). In Tcad-KO mice, pressure overload substantially increased heart size, to a level comparable to APN-KO hearts. Measurements of the heart weight/body weight (HW/BW) ratio and echocardiography documented this phenotype (Figure 3, B and C). M-mode analyses showed increased diastolic LV posterior wall thickness (LVPWd) in both Tcad-KO and APN-KO mice compared with WT animals (Figure 3D and Supplemental Table 1). LVPWd was unchanged after sham operation. To assess hypertrophy at the single-cell level, we measured cross-sectional areas of cardiomyocytes in the free wall of the LV. This analysis revealed increased hypertrophy of Tcad-KO and APN-KO cardiomyocytes compared with WT, in accordance with the increased HW/BW ratios and LVPWd measurements (Figure 3, E and F). Whereas myofiber cross-sectional area was enhanced after TAC in WT mice, there was a further significant increase in Tcad-KO and APN-KO hearts (Figure 3, E and F). Notably, we identified no decline in contractility, as measured by fractional shortening, after 7 days of TAC in the mutants compared with WT controls (Supplemental Table 1). Despite the exaggerated hypertrophy, this is consistent with the well-compensated early response to pressure overload.

Increased afterload and compensatory hypertrophy leads to elevated mechanical strain on the contractile apparatus and the intercalated disks. The cadherin family protein N-cadherin is prominently expressed in the heart and located at these junctions (32, 33). Testing N-cadherin protein levels and distribution at the intercalated disks, however, yielded no differences between Tcad-KO and WT mice in our study (Supplemental Figure 2). Moreover, 7 days of TAC did not result in changes of N-cadherin expression (Supplemental Figure 2). We therefore conclude that lack of T-cadherin causes no primary defect with regard to N-cadherin expression and distribution.

Experimental models have shown that APN's cardioprotective effects are mediated, at least in part, through AMPK (31, 34). We therefore probed the activation of AMPK in WT, Tcad-KO, and APN-KO myocardial lysates by determining phosphorylation of Thr-172 of the AMPKα subunit 1/2 with a phospho-specific antibody 7 days after TAC. AMPK phosphorylation was significantly reduced in Tcad-KO and APN-KO compared with WT hearts (Figure 3, G and H), which demonstrated that a common signaling pathway was activated by both T-cadherin and APN.

Accelerated decompensation in Tcad-KO and APN-KO hearts 4 weeks after TAC. The compensated phase of cardiac hypertrophy is typically followed by a decompensatory decline in heart function that is associated with ventricular dilation, reduced vascularization, and cardiomyocyte apoptosis (35). To test the role of T-cadherin in relation to APN during extended exposure to pressure overload, we subjected WT, Tcad-KO, and APN-KO mice to 4 weeks of TAC. Again, we noted exaggerated hypertrophy in the mutants (Figure 4, A and B) that, in this model, was accompanied by increased numbers of apoptotic cells in the myocardium (Figure 4C).

Myocardial vascularization is a critical determinant of heart function during the hypertrophic response (35). The physiological balance between capillary density and heart growth characterizes compensated hypertrophy, whereas decompensated hypertrophy (considered bad) is associated with reduced vascularization. Recently, the requirement of APN for the angiogenic supply during the long-term response to TAC was demonstrated (36). As both

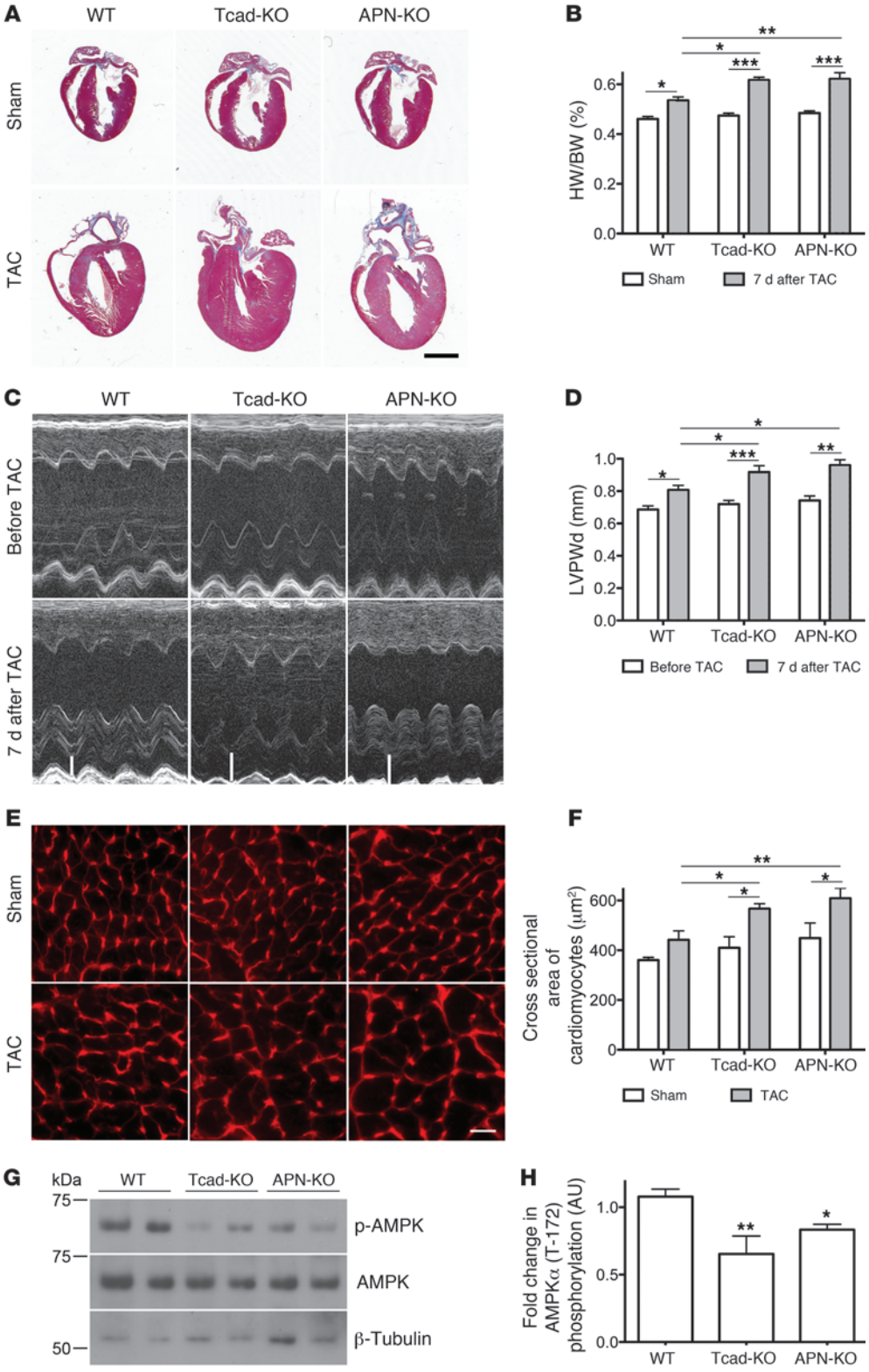

Figure 3

Exaggerated cardiac hypertrophy and reduced AMPK phosphorylation in Tcad-KO and APN-KO mice after 7 days of TAC. (**A**) Representative images of trichrome-stained WT, Tcad-KO, and APN-KO hearts 7 days after sham or TAC surgery. Scale bar: 2 mm. (**B**) HW/BW ratio. n = 8 (WT); 7 (Tcad-KO); 11 (APN-KO). (**C**) M-mode echocardiograms from WT, Tcad-KO, and APN-KO mice 7 days after TAC surgery. White bars indicate diastolic LV wall thickness after TAC. (**D**) Quantification of LVPWd before and 7 days after TAC surgery. n = 10 (WT); 14 (Tcad-KO); 5 (APN-KO). (**E**) Fluorescent wheat germ agglutinin–stained cell surfaces in hearts from WT, Tcad-KO, and APN-KO mice 7 days after sham or TAC surgery. Scale bar: 10 μm. (**F**) Quantification of myocyte cross-sectional areas in **E**. n = 3 (sham) or 4 (TAC) per group. (**G**) Representative immunoblots from WT, Tcad-KO, and APNKO myocardial lysates 7 days after TAC using phospho-specific (Thr-172) and total anti-AMPK antibodies with reference to β-tubulin. (**H**) Quantification of phospho-AMPK/total AMPK ratio in **G**. n = 5 (WT and APN-KO); 4 (Tcad-KO). $^*P < 0.05$, $^{**}P < 0.01$, $^{***}P < 0.001$ versus WT or as indicated by brackets.

T-cadherin and APN exert proangiogenic functions in mammary tumors (29, 37, 38), we tested capillary vessel density in the interventricular septum 7 days and 28 days after TAC. Consistent with an early well-compensated hypertrophic response, at 7 days o overt differences in vascularization were observed among WT, Tcad-KO, and APN-KO mice (Supplemental Figure 3).

In line with an exaggerated decompensated hypertrophic response at 28 days, myocardial capillary density was reduced

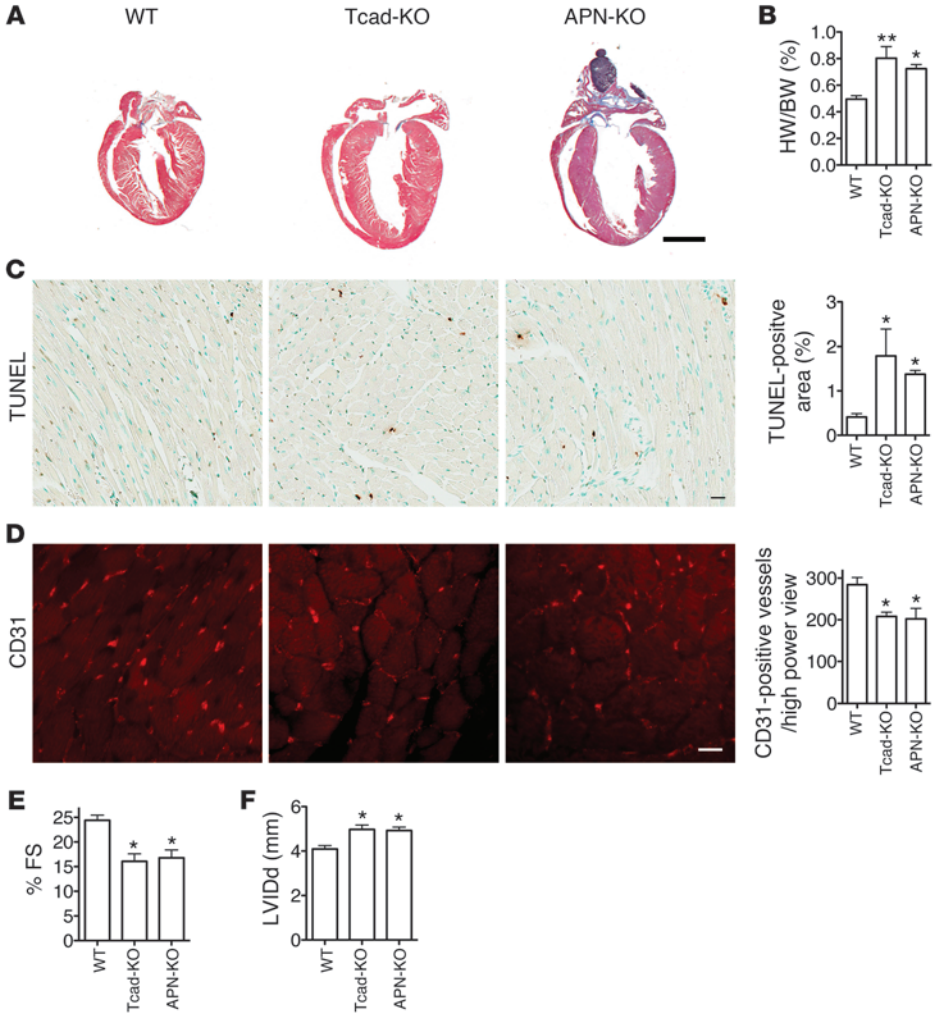

Figure 4
Long-term TAC leads to dilation and reduced contractility in Tcad-KO and APN-KO hearts. (**A**) Representative images of trichrome-stained WT, Tcad-KO, and APN-KO hearts 28 days after TAC surgery. Scale bar: 2 mm. (**B**) HW/BW ratios. (**C**) Representative images from TUNEL-stained heart sections in WT, Tcad-KO, and APN-KO hearts, with quantification of TUNEL-positive area of whole heart sections. Scale bar: 20 μm. (**D**) Representative images of CD31-stained heart sections. Quantification was carried out in the free wall of the LV by counting number of capillaries per high-power field. Scale bar: 5 μm. (**E**) Fractional shortening (FS) was significantly reduced in Tcad-KO and APN-KO animals. (**F**) LV inner diameter in diastole (LVIDd) was significantly increased in Tcad-KO and APN-KO mice. (**B**–**F**) $n = 4$ (WT and Tcad-KO); 3 (APN-KO). $^*P < 0.05$, $^{**}P < 0.01$ versus WT.

in APN-KO mice, as previously reported (36). In Tcad-KO mice, a similar decrease in vascularization was evident (Figure 4D). In agreement, the mutant hearts undergoing 4 weeks of TAC were characterized by reduced contractility, as measured by fractional shortening, and showed dilation of the LV (Figure 4, E and F). These combined data indicated that both Tcad-KO and APN-KO mice undergo an overshooting hypertrophic response during aortic banding. T-cadherin and APN appear to protect both from exaggerated hypertrophy in the short term and from severe decompensation during extended challenge.

Rescue of the hypertrophic phenotype with recombinant APN depends on T-cadherin. The above findings led us to predict that interaction of T-cadherin with APN mediates cardioprotection. Adenovirus-expressed recombinant APN (adAPN) reverts the exacerbated cardiac hypertrophy of APN-KO mice (31). Our finding of low T-cadherin expression levels in APN-KO hearts (Figure 1, A and B) predicted a mechanism whereby adAPN upregulates T-cadherin expression in the myocardium to enable docking of adAPN to cardiomyocytes. To test this model, we investigated whether adAPN treatment restored T-cadherin protein expression in APN-KO hearts. APN-KO mice were injected through the tail vein with 2×10^8 PFU adAPN-encoding or control adGPF-encoding virus and were sacrificed after 10 days. adAPN treatment of APN-KO mice increased circulating adAPN levels to physiological levels at an average of 11.6 μg/ml (Supplemental Table 2). Examination of hearts from adGFP-treated APN-KO mice showed near-background T-cadherin protein levels (Figure 5A), comparable to Figure 1A. In contrast, treatment with adAPN yielded robust T-cadherin reexpression by cardiomyocytes in APN-KO mice, and the ectopically expressed adAPN colocalized with T-cadherin (Figure 5A). Cardiac T-cadherin mRNA levels remained unchanged in APN-KO mice regardless of treatment (Figure 5B), consistent with the notion that regulation of T-cadherin expression occurs posttranscriptionally.

To directly test the requirement of T-cadherin in limiting cardiac hypertrophy through interaction with APN, we generated mice deficient in both T-cadherin and APN gene expression (T-cadherin/APN double-KO; referred to herein as DKO). This was necessary because Tcad-KO mice displayed high APN serum levels (Figure 1D) that would confound the interpretation of adAPN supplementation experiments. adAPN- or adGFP-encoding virus was injected into APN-KO and DKO mice 3 days before TAC surgery, and animals were sacrificed 7 days after surgery. APN-KO and DKO mice treated with control adGFP showed exaggerated cardiac hypertrophy after TAC, comparable to that in the above experiments with APN-KO and Tcad-KO mice. No enhanced effect resulted from the double mutation (Figure 6, A–D). Consistent

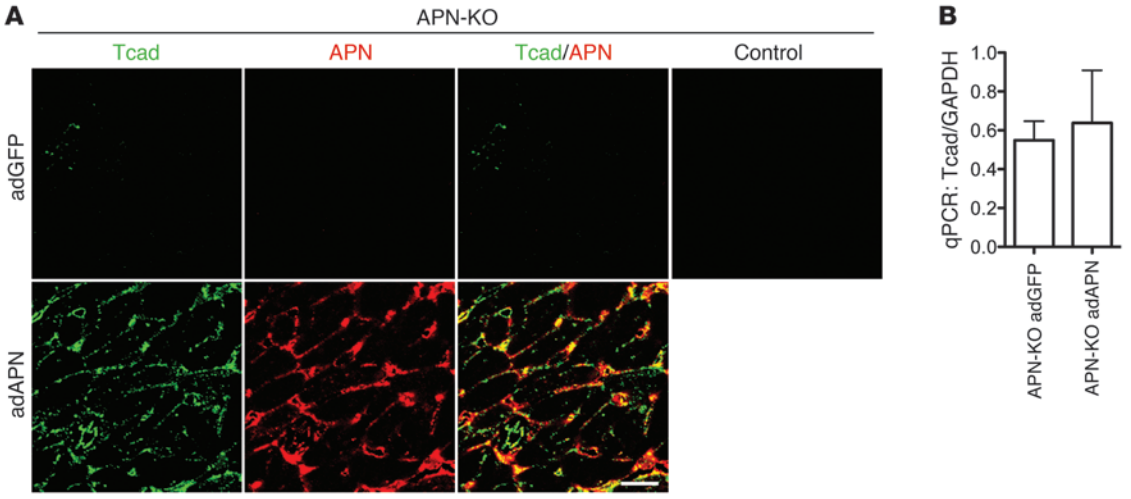

Figure 5
T-cadherin reexpression in APN-KO hearts after adAPN treatment. (**A**) Immunostaining of heart sections from adGFP- or adAPN-treated APN-KO mice with T-cadherin and APN antibodies. Control staining confirmed absence of GFP signals in the heart. Scale bar: 5 μm. (**B**) Cardiac T-cadherin mRNA levels measured by qPCR in adGFP- (n = 5) or adAPN-treated (n = 3) APN-KO mice.

with previous reports, adAPN-treatment neutralized the exaggerated hypertrophy after TAC in APN-KO mice (Figure 6, A–D) and yielded only a modest hypertrophic response compared with the sham condition (Figure 6B). In contrast, adAPN treatment of DKO animals failed to reverse the exaggerated cardiac hypertrophic response, and hearts remained enlarged, as in the control adGFP-treated APN-KO and DKO conditions (Figure 6, A–D). To corroborate these findings, we investigated the activation of APMK 7 days after TAC. In adAPN-treated APN-KO mice, cardiac AMPKα phosphorylation was enhanced compared with adGFP-treated controls (Figure 6, E and F). In contrast, there was no increase in phospho-AMPKα in the DKO condition. To confirm this activating phosphorylation of AMPK, we analyzed the phosphorylation status of the AMPK substrate acetyl-CoA-carboxylase (ACC). ACC showed corresponding Ser-79 phosphorylation in adAPN-treated APN-KO mice, whereas no increase was observed in the DKO condition (Figure 6, E and G). These data suggest that T-cadherin limits cardiac hypertrophy through APN-mediated activation of the AMPK signaling pathway.

T-cadherin is required for APN-mediated protection from myocardial ischemia-reperfusion injury. The role of T-cadherin and APN in hypertrophy points to a general cardioprotective function. Myocardial infarction represents an acute lethal cardiac pathology, and APN displays protective properties in mouse models (39, 40). To test the role of T-cadherin in this severe paradigm for cardiac stress, we subjected WT, Tcad-KO, and APN-KO mice to ischemia-reperfusion. The left anterior descending artery was ligated for 30 minutes, followed by 48 hours of reperfusion. Heart cross-sections revealed significantly increased necrotic area in both Tcad-KO and APN-KO mice as well as in the DKO mutants (Figure 7A). The infarct area/area at risk (IA/AAR) and IA/LV area ratios were significantly enhanced in Tcad-KO, APN-KO, and DKO mice, while the AAR/LV area ratio was the same (Figure 7B). Treatment with adAPN reduced infarct size in APN-KO mice, as previously reported (40), while this treatment was ineffective in the DKO mutants (Figure 7, A and B). As AMPK activation protects the heart from ischemia-reperfusion injury (40), we tested AMPK phosphorylation in the at-risk regions of the myocardium. Similar to the results after TAC, we found reduced AMPK phosphorylation in Tcad-KO and APN-KO compared with WT tissue (Figure 7C). To assess whether the APN-KO and Tcad-KO mutation reduced protection from apoptosis, we analyzed the areas adjacent to the infarcts by TUNEL assay. Consistent with the increased stress, we found an enhanced apoptotic index in both Tcad-KO and APN-KO hearts (Figure 7D). These combined data lead us to conclude that T-cadherin in conjunction with APN protects the heart from multiple stressors, such as chronically increased afterload and myocardial ischemia.

Discussion

This investigation into T-cadherin's function in the heart — the first to our knowledge — establishes a role in APN-dependent cardioprotection during chronic and acute stress. We showed that T-cadherin deficiency resulted in exacerbated cardiac hypertrophy during chronic pressure overload and aggravated acute ischemia-reperfusion injury. Parallel experiments with APN-KO mice show similar phenotypes (31, 40) and validate all procedures. Our data established that T-cadherin expressed by cardiomyocytes is necessary for sequestering APN to the heart. Correspondingly, ablation of T-cadherin expression dramatically increased levels of APN in the circulation. This excessive amount of APN was unable to associate with cardiac tissue and activate APN-dependent cardiac AMPK signaling, a major pathway associated with cardioprotective functions. APN-KO mice were characterized by low cardiac T-cadherin protein expression. Administration of recombinant APN to APN-KO mice rescued the cardiac phenotype by restoring T-cadherin expression by cardiomyocytes to physiological levels. This reestablished cardiac APN association, thereby reactivating AMPK signaling and limiting exacerbated cardiac injury. The same treatment failed to rescue the phenotype in the absence of T-cadherin. Thus, T-cadherin expressed on cardiomyocyte surfaces is necessary for binding APN and thereby enabling its cardioprotective functions.

Cardiac hypertrophy caused by pressure overload leads to an initial compensatory phase of cardiomyocyte growth that maintains resting output (41). Prolonged hypertrophy, however, results in

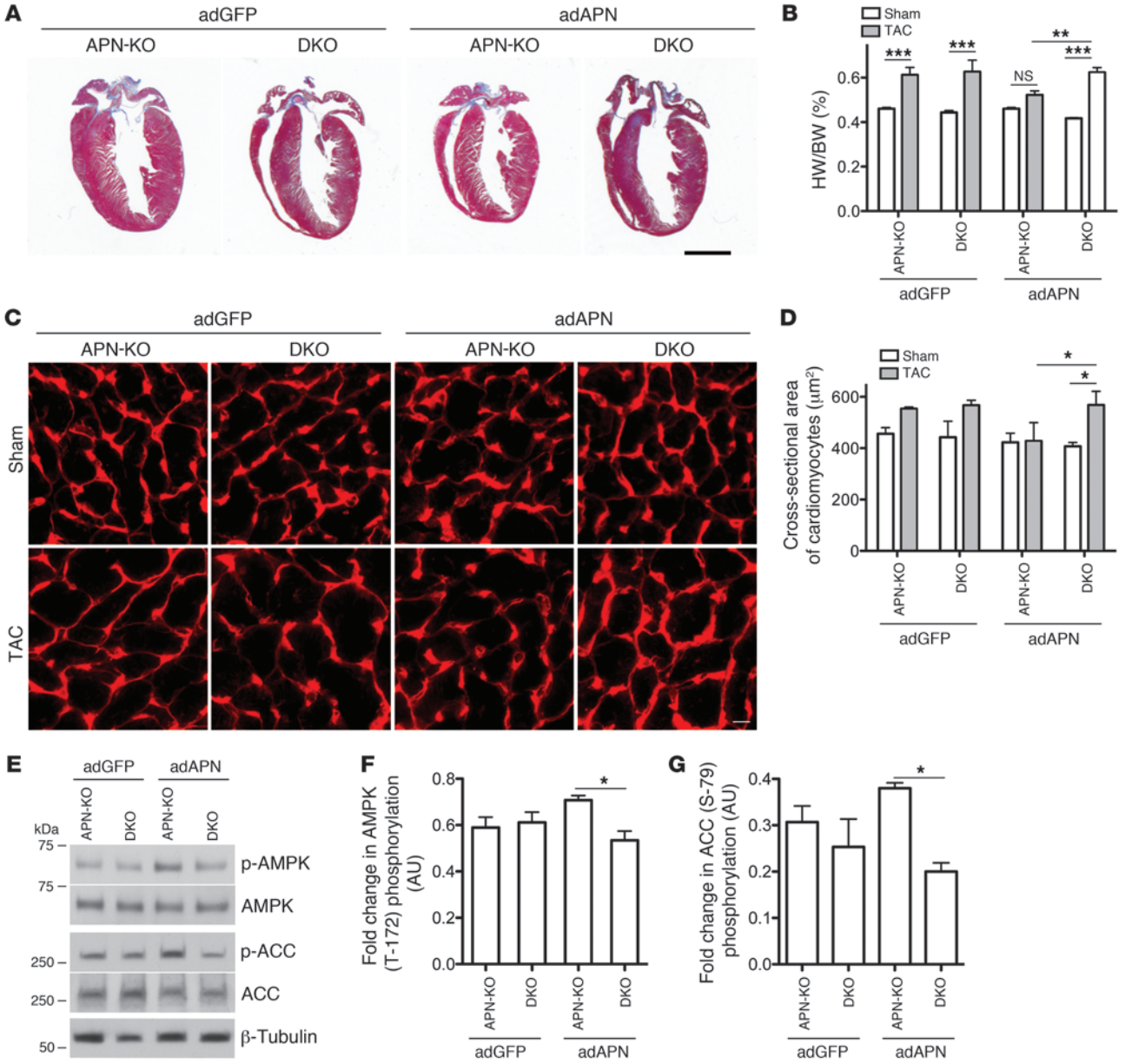

Figure 6

Reversion of exaggerated cardiac hypertrophy phenotype in APN-KO depends on T-cadherin. (**A**) Representative trichrome-stained heart sections 7 days after TAC. Scale bar is 2 mm. (**B**) HW/BW ratios in adGFP- or adAPN-treated APN-KO and DKO mice after sham or TAC surgery. (**C**) Representative images of wheat germ agglutinin–stained myocardium to reveal cardiomyocyte cross-sectional area, quantified in **D**. Scale bar: 5 μm. (**E**) Representative immunoblots showing cardiac AMPK and ACC phosphorylation in adGFP- or adAPN-treated APN-KO and DKO animals 7 days after TAC. (**F** and **G**) Quantification of phospho-AMPK/total AMPK and phospho-ACC/total ACC ratios. (**B**, **D**, **F**, and **G**) $n = 3$ (adGFP) or 4 (adAPN) per group. $^*P < 0.05$, $^{**}P < 0.01$, $^{***}P < 0.001$.

decompensation associated with ventricular dilation and progressive decline in cardiac function that can lead to heart failure (35). We observed exacerbated hypertrophy at both early and late stages in Tcad-KO mice in parallel with similar defects in mice lacking APN. At 7 days after aortic banding, the compensated hypertrophic response showed increased LV posterior wall thickness with normal functional parameters (Figure 3 and Supplemental Table 1). After prolonged pressure overload (28 days), both mutants displayed LV dilation and declined heart function that was accompanied by decreased capillary density and increased apoptotic cell death (Figure 4 and Supplemental Table 3).

Vascularization plays an important role in maintaining the compensated hypertrophic response. Accordingly, during the early compensatory phase of hypertrophy during pressure overload, we observed no changes in myocardial vascularization in Tcad-KO or APN-KO compared with WT mice. Thus, increased LV wall thickness in conjunction with downregulation of AMPK signaling appears to be a cardiomyocyte autonomous response. Dur-

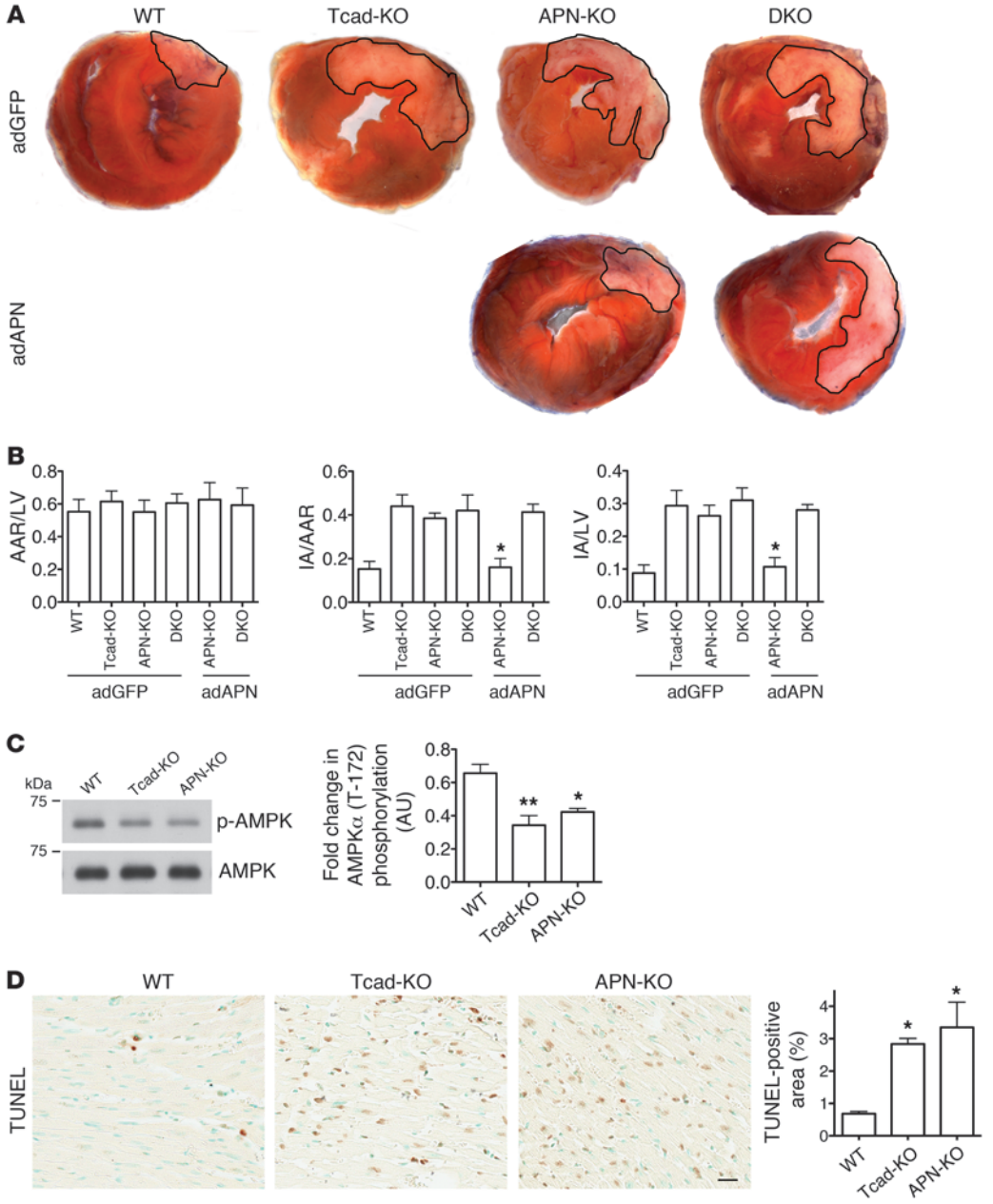

Figure 7

T-cadherin is required for APN-mediated protection against ischemia-reperfusion. (**A**) Representative images of myocardial tissue sections 48 hours after ischemia-reperfusion. Outlined white areas indicate IA, red color indicates AAR. (**B**) Quantification of infarct size by AAR/LV area, IA/AAR, and IA/LV ratios. $n = 4$ (adGFP-treated WT, Tcad-KO, and DKO and adAPN-treated DKO); 6 (adGFP-treated APN-KO); 3 (adAPN-treated APN-KO). *$P < 0.05$ versus adGFP-treated Tcad-KO, APN-KO, and DKO and adAPN-treated DKO. (**C**) Representative immunoblots from WT, Tcad-KO, and APN-KO myocardial lysates of ischemic areas 48 hours after ischemia-reperfusion using phospho-specific (Thr-172) and total anti-AMPK antibodies. Quantification of phospho-AMPK/total AMPK ratios ($n = 3$ per group). (**D**) Representative images of TUNEL-stained heart sections. Scale bar: 20 μm. TUNEL-positive area was analyzed in regions adjacent to IAs ($n = 3$ per group).*$P < 0.05$, **$P < 0.01$ versus WT.

ing the decompensating phase of cardiac hypertrophy, however, we observed decreased capillary density associated with attenuated cardiac function in both Tcad-KO and APN-KO mice. This is consistent with recent studies reporting that prolonged pressure overload diminishes cardiac capillary density in APN-KO mice by decreasing cardiomyocyte production of VEGF and AMPK signaling (36). We previously identified a proangiogenic function for T-cadherin in the mouse mammary tumor virus–induced polyoma virus middle T (MMTV-PyV-mT) model of mammary cancer and ischemic retinal angiogenesis (29). Similarly, APN is known to promote ischemia-induced neovascularization in MMTV-PyV-mT mouse mammary tumors (37, 38) and in the ischemic hindlimb (42). This raises the possibility that the association between APN and T-cadherin modulates the hypertrophic response through

adaptive endothelial cell–mediated cardiac angiogenesis in addition to exerting functions in cardiomyocytes. Evaluation of the cell type–specific contributions of T-cadherin is therefore an important task for future studies.

Ischemia-reperfusion injury is a model for acute cardiac infarction in which APN exerts a protective role (40). Here we revealed the strict requirement for T-cadherin in this process in the mouse model. APN deficiency suppressed T-cadherin expression by cardiomyocytes, and administration of recombinant adAPN led to the reexpression of T-cadherin, allowing adAPN binding and rescue of the cardiac phenotype in APN-KO mice. Absence of T-cadherin disabled this rescue. These findings suggest that the heart reversibly responds to APN levels in the circulation by regulating T-cadherin levels and support the conclusion that T-cadherin is essential for the cardiac localization and rescue activity of adAPN. The crucial role of T-cadherin was further emphasized by the finding that supraphysiological APN serum concentrations in the Tcad-KO mice were ineffective in cardioprotection.

Some readers may ask why sudden cardiac death can occur in young athletes despite presumably high APN levels. Although this area is insufficiently studied, the most common known cause of rare and sudden cardiac arrest under 35 years is hypertrophic cardiomyopathy, an autosomal-dominant trait most often associated with mutations in genes that code for sarcomere proteins (43, 44). Such inherent microstructural abnormalities of the heart often remain undisclosed until the occurrence of sudden cardiac death. Therefore, a likely explanation for the ineffectiveness of APN in protecting an athlete's heart is that the congenital defects of hypertrophic cardiomyopathy dominate over APN-mediated cardioprotection, or that mutations occur that render APN inactive. In this context, it will be interesting to investigate deceased athletes' hearts for T-cadherin and associated pathways. However, heart disease mostly occurs in the absence of mutations and is associated with increased age and altered metabolic status. An array of epidemiological and clinical data suggests that APN confers potent endogenous protection in these cases (11, 12, 45, 46).

How does APN mediate tissue-specific functions in the heart? T-cadherin is expressed in cardiomyocyte membrane microdomains that are visible as discrete puncta by immunohistochemistry. APN showed a strikingly overlapping pattern (Figure 1), in line with the association of these molecules. That this interaction is direct is supported by 2 lines of in vitro evidence: first, T-cadherin was precipitated from differentiated C2C12 myotubes with APN antibodies after treatment with HMW APN (Figure 2A); and second, ectopic expression of T-cadherin in HEK293 cells was sufficient for binding serum APN (Figure 2B).

Although T-cadherin is effective in binding APN and activating its downstream signaling target AMPK, it falls short of being a receptor that both binds and transduces the binding signal to intracellular signaling pathways: T-cadherin's glycosyl phosphatidylinositol anchor precludes direct interactions with intracellular signaling adaptors. Thus, we envision T-cadherin in association with transmembrane proteins that in turn associate with intracellular adaptor proteins to activate APN signaling targets. One possible mechanism is that T-cadherin exerts cardioprotection through activating AMPK via the integrin pathway. Integrin levels are modulated by T-cadherin (47), and ectopic expression of T-cadherin in cultured endothelial cells is reported to activate integrin-linked kinase (ILK) signaling (48). In turn, ILK activation is implicated with AMPK signaling to protect the heart from LV hypertrophy (49).

Alternatively, and perhaps more likely, AdipoR1 or -R2 are strong candidates to associate with or work in concert with T-cadherin as they (a) are activated in an APN-dependent manner; (b) serve upstream of AMPK signaling (17); and (c) are expressed the heart and thus implicated in cardiomyocyte functions (13, 50). Support for involvement of AdipoR1 in T-cadherin/APN-dependent signaling comes from a recent paper that describes the skeletal muscle–specific inactivation of AdipoR1 (15). In these mice, APN fails to regulate muscle metabolism, including AMPK activation. As T-cadherin is abundant in normal skeletal muscle and responsible for APN binding, it is conceivable that the cooperation between T-cadherin and AdipoR1 enables APN functions in both skeletal and cardiac muscle. Indeed, consistent with published work (13), we established AdipoR1 and -R2 mRNA and protein expression in the myocardium. However, unlike T-cadherin, cardiac expression levels of AdipoR1 and -R2 were independent of APN serum concentrations and remained unaltered between APN-KO and Tcad-KO mice. The continued expression of AdipoR1 and -R2 in Tcad-KO mice, combined with the absence of cardiac APN association, suggests that these receptors alone are insufficient to enable binding and thereby cardioprotective functions of APN. We provide experimental evidence for this suggestion by our demonstration that T-cadherin ectopically expressed in HEK293 cells effectively bound APN, whereas surface expression of AdipoR1 and -R2 in the same cells alone yielded no detectable association of serum APN (Figure 2B). These data thus support a model in which physical association of APN with T-cadherin is a prerequisite for APN's physiological activity in the heart, and suggest that a possible function of AdipoR1/R2 is secondary to the binding of APN to T-cadherin.

In summary, we identified the critical physiological function of T-cadherin in sequestering APN to the myocardium and enabling APN's protective functions in cardiac injury models in the mouse. Combined with the current literature, our data are consistent with a model in which T-cadherin serves the APN-binding function while yet-unknown transmembrane proteins, possibly including AdipoR1 or -R2, are required for transmitting the binding signal to intracellular signaling pathways. Clearly, more research is necessary to determine the molecular mechanism by which APN exerts its cardioprotective functions, including studies with AdipoR1/R2 KO mice. Our present study contributes insights into the biology of APN by identifying T-cadherin as a physiological APN-binding receptor that enables the association of APN with the heart. This work opens the possibility for a role of T-cadherin in other physiological processes that are modulated by APN.

Methods

Mice. The IACUC of Sanford-Burnham Medical Research Institute approved our study protocols. C57BL/6 Tcad-KO mice were previously described (29). C57BL/6 APN-KO mice were provided by N. Maeda, T. Funahashi, and Y. Matsuzawa (Osaka University, Osaka, Japan; ref. 30). Animals were fed with a normal diet.

TAC. 8- to 12-week-old male C57BL/6 WT, Tcad-KO, APN-KO, or DKO mice were anesthetized with ketamine (100 mg/kg) and xylazine (10 mg/kg). The chest cavity was entered by blunt dissection of the second intercostal space at the left upper sternal border, and the transverse aorta was isolated. TAC was achieved by tying a 7-0 nylon suture ligature against a 26- to 27-gauge needle and the aorta and subsequent removal of the needle. Sham-operated mice underwent the same surgical procedure without constriction of the aorta. Transthoracic echocardiography was done before TAC and 7 or 28 days after TAC.

Ischemia-reperfusion injury. 8- to 12-week-old male C57BL/6 WT, Tcad-KO, APN-KO, or DKO mice were anesthetized as described above. The chest cavity was entered by blunt dissection of the fourth intercostal space, 2 mm away from the left sternal border. Opening the pericardial sac exposed the heart. The left anterior descending artery was ligated with a 6-0 silk suture about 1–2 mm beneath the tip of the left auricle. After 30 minutes of coronary occlusion, the ligation was opened, and the lungs were reinflated with a small catheter left in the thorax to evacuate air and fluids. The chest cavity was closed, and the mouse was extubated and maintained on high oxygen during recovery from the surgery.

Determination of AAR and IA. 48 hours after ischemia-reperfusion surgery, mice were anesthetized, and the left anterior descending artery was reoccluded. 0.5 ml of a 1% Evans blue (Sigma-Aldrich) solution was injected into the LV to mark the nonischemic tissue. The heart was then excised, washed in PBS, and cut into 4 transverse slices, which were subsequently stained in 2% 2,3,5-triphenyltetrazolium chloride (Sigma-Aldrich) for 15 minutes at room temperature to aid visualization of the IA. Digital images of heart sections were analyzed for LV area, AAR, and necrotic area using Image J software.

Adenovirus-mediated gene transfer. We injected 2×10^8 PFU of adAPN (31) or adGFP (provided by M. Mercola; Sanford-Burnham Medical Research Institute) into the tail vein of mice 3 days prior to TAC. GFP fluorescence was verified in the liver. APN was detected in the circulation using Western blotting and ELISA (R&D).

Immunohistochemistry. Heart sections were sequentially treated with Target Retrieval Solution (Dako), 1% Saponin (Fluka), and saturated Sudan Black (MPBio) in 70% ethanol; blocked with Antibody Diluent (Dako); and incubated with APN (R&D and PA1-054, Affinity Bioreagents), N-cadherin (BD Biosciences), Connexin 43 (Millipore), CD31 (BD Biosciences), or T-cadherin (ref. 29 and R&D) antibodies. Alexa Fluor 488, Alexa Fluor 647, and Alexa Fluor 594 fluorescent conjugates (Invitrogen) were used to detect the respective primary antibodies. Negative controls were tissues from KO animals or slides processed in parallel without primary antibody. Before CD31 staining, sections were digested with 0.1% trypsin (Zymed). Apoptotic cells were identified by TUNEL (Millipore). TUNEL-stained sections were counterstained with methyl green. Immunofluorescent images were taken with a Fluoview confocal microscope (Olympus).

Histology. Deparaffinized heart sections were used for Trichrome staining. Frozen heart sections were fixed in acetone and processed for staining with fluorescently labeled wheat germ agglutinin (Sigma-Aldrich).

Tissue culture. C2C12 myoblasts were maintained in DMEM (Cellgro) with 20% FCS (Gibco, Invitrogen) and differentiated in DMEM with 2% horse serum (Gibco, Invitrogen). HEK293 cells were maintained in DMEM with 10% FCS. Stable HEK293 lines were generated by infection with a retroviral vector (pL-N1 or pL–T-cadherin) and subsequent selection. Transient transfection of HEK293 cells with the HA-tagged AdipoR1 and Flag-tagged AdipoR2 constructs (provided by M.-H. Lee and L.M. Luttrell, University of South Carolina, Charleston, South Caroline, USA; ref. 51) was done by calcium phosphate method, and surface expression of AdipoR1 and -R2 was verified by surface biotinylation and immunostaining (data not shown).

Cardiomyocyte isolation. Adult mouse cardiomyocytes were isolated using the Neomyt Kit (Cellutron Life Technologies) according to the manufacturer's protocol. Sequential plating ensured cardiomyocyte purity.

Immunoprecipitation. C2C12 cells were incubated with HMW APN (provided by L. Shapiro, Columbia University, New York, New York, USA) and cross-linked with 2.5 mmol/l dimethyl 3,3′-dithiopropionimidate dihydrochloride (Sigma-Aldrich) for 30 minutes at room temperature. Cells were then washed and lysed with lysis buffer (20 mmol/l Tris HCl pH 7.4, 150 mmol/l NaCl, 1 mmol/l EDTA, 10 mmol/l sodium pyrophosphate, 10 mmol/l beta glycerophosphate, 50 mmol/l sodium fluoride, protease inhibitor cocktail [Sigma-Aldrich], 0.1 mmol/l PMSF, and 1% NP40), and incubated with either normal rabbit IgG or anti-APN antibodies at 4°C for 1 hour. Magnetic Protein A beads (Invitrogen) were then added, and the samples were further incubated at 4°C for 1 hour. The beads were then collected and washed 5 times in lysis buffer. Bound protein complexes were analyzed by Western blotting.

Western blotting. Snap-frozen heart tissue was mechanically dissociated and suspended in lysis buffer. Proteins were separated by reducing SDS-PAGE and transferred to PVDF membranes. Membranes were then incubated with specific antibodies to APN, T-cadherin (29), N-cadherin, AdipoR1 (Abcam), AdipoR2 (Phoenix Pharmaceuticals), β-tubulin (Chemicon), phospho-AMPKα (Thr-172) (Cell Signaling), AMPKα (Cell Signaling), phospho-ACC (Ser-79) (Upstate), ACC (Upstate), or the Flag (Sigma-Aldrich) and HA tags (Roche).

Real-time qPCR. Total RNA was extracted using TRIzol (Invitrogen) from heart tissue or cultured cells. Equal amounts were reverse transcribed using oligo $(dT)_{18}$ and random hexamer primers (Transcriptor First Strand cDNA Synthesis Kit; Roche). Real-time qPCR analysis was performed with SYBR green. T-cadherin (5′-CATCGAAGCTCAAGATATGG-3′; 5′-GATTTCCATTGATGATGGTG-3′), AdipoR1 (5′-ACACAGAGACTGGCAACATC-3′; 5′-GAGCAATCCCTGAATAGTCC-3′), and AdipoR2 (5′-TGGACACATCTCCTAGGTTG-3′; 5′-TAGAGAAGAGTCGGGAGACC-3′) cDNAs were detected and normalized to GAPDH (5′-CCAGTATGACTCCACTCACG-3′; 5′-GACTCCACGACATACTCAGC-3′).

Statistics. Statistical analysis was done using Prism software by 1-way ANOVA with Bonferroni post-tests. A P value less than 0.05 was considered significant. Values are mean ± SEM.

Note added in proof. A recent genome-wide association study establishes a further strong link of *Cdh13* to APN levels in Asian populations (52).

Acknowledgments

We gratefully acknowledge Robbin Newlin and her team (Histology and Molecular Pathology Facility, Sanford-Burnham Medical Research Institute, SBMRI) for expert histology assistance, Edward Monosov (Cell Imaging Facility, SBMRI) for help with fluorescence imaging, Francisco Beltran and Adriana Charbono (Animal Facility, SBMRI) for animal care, and Regina Kapono for assistance with the manuscript. Norikazu Maeda, Tohru Funahashi, and Yuji Matsuzawa provided the APN-KO mice; Mi-Hye Lee and Louis M. Luttrell made available the tagged AdipoR1 and -R2 constructs; Lawrence Shapiro provided the recombinant HMW APN. We thank Vincent Chen and Ramon Diaz (SBMRI) for insightful discussions. The Sanford-Burnham Cancer Center Core Grant–funded Animal-, Histopathology-, and Cell Imaging Core Facilities and an institutional pilot grant supported this project. M.S. Denzel was supported for this thesis work by a fellowship from the Boehringer Ingelheim Fonds. M.-C. Scimia was a CIRM Clinical Fellow. This work was funded by NIH grant HL102680 and the American Heart Association (to B. Ranscht), NIH grants HL065484 and HL086879 (to P. Ruiz-Lozano), and NIH grants AG15052 and HL68758 (to K. Walsh).

Received for publication April 23, 2010, and accepted in revised form September 8, 2010.

Address correspondence to: Barbara Ranscht, Sanford-Burnham Medical Research Institute, 10901 North Torrey Pines Road, La Jolla, California 92037, USA. Phone: 858.646.3122; Fax: 858.646.3197; E-mail: ranscht@sanfordburnham.org.

1. Prasad A, Stone GW, Holmes DR, Gersh B. Reperfusion injury, microvascular dysfunction, and cardioprotection: the "dark side" of reperfusion. *Circulation*. 2009;120(21):2105–2112.
2. Lorell BH, Carabello BA. Left ventricular hypertrophy: pathogenesis, detection, and prognosis. *Circulation*. 2000;102(4):470–479.
3. Artham SM, Lavie CJ, Milani RV, Patel DA, Verma A, Ventura HO. Clinical impact of left ventricular hypertrophy and implications for regression. *Prog Cardiovasc Dis*. 2009;52(2):153–167.
4. Eisenberg MS, Mengert TJ. Cardiac resuscitation. *N Engl J Med*. 2001;344(17):1304–1313.
5. Rogers WJ, et al. Temporal trends in the treatment of over 1.5 million patients with myocardial infarction in the US from 1990 through 1999: the National Registry of Myocardial Infarction 1, 2, and 3. *J Am Coll Cardiol*. 2000;36(7):2056–2063.
6. Arita Y, et al. Paradoxical decrease of an adipose-specific protein, adiponectin, in obesity. *Biochem Biophys Res Commun*. 1999;257(1):79–83.
7. Hu E, Liang P, Spiegelman BM. AdipoQ is a novel adipose-specific gene dysregulated in obesity. *J Biol Chem*. 1996;271(18):10697–10703.
8. Shibata R, Ouchi N, Murohara T. Adiponectin and cardiovascular disease. *Circ J*. 2009;73(4):608–614.
9. Chen MP, et al. Hypoadiponectinemia is associated with ischemic cerebrovascular disease. *Arterioscler Thromb Vasc Biol*. 2005;25(4):821–826.
10. Iwashima Y, et al. Hypoadiponectinemia is an independent risk factor for hypertension. *Hypertension*. 2004;43(6):1318–1323.
11. Kumada M, et al. Association of hypoadiponectinemia with coronary artery disease in men. *Arterioscler Thromb Vasc Biol*. 2003;23(1):85–89.
12. Hong SJ, Park CG, Seo HS, Oh DJ, Ro YM. Associations among plasma adiponectin, hypertension, left ventricular diastolic function and left ventricular mass index. *Blood Press*. 2004;13(4):236–242.
13. Yamauchi T, et al. Cloning of adiponectin receptors that mediate antidiabetic metabolic effects. *Nature*. 2003;423(6941):762–769.
14. Bjursell M, et al. Opposing effects of adiponectin receptors 1 and 2 on energy metabolism. *Diabetes*. 2007;56(3):583–593.
15. Iwabu M, et al. Adiponectin and AdipoR1 regulate PGC-1alpha and mitochondria by Ca(2+) and AMPK/SIRT1. *Nature*. 2010;464(7293):1313–1319.
16. Liu Y, et al. Deficiency of adiponectin receptor 2 reduces diet-induced insulin resistance but promotes type 2 diabetes. *Endocrinology*. 2007;148(2):683–692.
17. Yamauchi T, et al. Targeted disruption of AdipoR1 and AdipoR2 causes abrogation of adiponectin binding and metabolic actions. *Nat Med*. 2007; 13(3):332–339.
18. Hug C, Wang J, Ahmad NS, Bogan JS, Tsao TS, Lodish HF. T-cadherin is a receptor for hexameric and high-molecular-weight forms of Acrp30/adiponectin. *Proc Natl Acad Sci U S A*. 2004;101(28):10308–10313.
19. Ranscht B, Dours-Zimmermann MT. T-cadherin, a novel cadherin cell adhesion molecule in the nervous system lacks the conserved cytoplasmic region. *Neuron*. 1991;7(3):391–402
20. Vestal DJ, Ranscht B. Glycosyl phosphatidylinositol--anchored T-cadherin mediates calcium-dependent, homophilic cell adhesion. *J Cell Biol*. 1992;119(2):451–461.
21. Fredette BJ, Miller J, Ranscht B. Inhibition of motor axon growth by T-cadherin substrata. *Development*. 1996;122(10):3163–3171.
22. Ranscht B, Bronner-Fraser M. T-cadherin expression alternates with migrating neural crest cells in the trunk of the avian embryo. *Development*. 1991;111(1):15–22.
23. Fredette BJ, Ranscht B. T-cadherin expression delineates specific regions of the developing motor axon-hindlimb projection pathway. *J Neurosci*. 1994;14(12):7331–7346.
24. Ciatto C, et al. T-cadherin structures reveal a novel adhesive binding mechanism. *Nat Struct Mol Biol*. 2010;17(3):339–347.
25. Doyle DD, Goings GE, Upshaw-Earley J, Page E, Ranscht B, Palfrey HC. T-cadherin is a major glycophosphoinositol-anchored protein associated with noncaveolar detergent-insoluble domains of the cardiac sarcolemma. *J Biol Chem*. 1998; 273(12):6937–6943.
26. Ling H, et al. Genome-wide linkage and association analyses to identify genes influencing adiponectin levels: the GEMS Study. *Obesity (Silver Spring)*. 2009;17(4):737–744.
27. Org E, et al. Genome-wide scan identifies CDH13 as a novel susceptibility locus contributing to blood pressure determination in two European populations. *Hum Mol Genet*. 2009;18(12):2288–2296.
28. Kraja AT, et al. QTLs of factors of the metabolic syndrome and echocardiographic phenotypes: the hypertension genetic epidemiology network study. *BMC Med Genet*. 2008;9:103.
29. Hebbard LW, Garlatti M, Young LJ, Cardiff RD, Oshima RG, Ranscht B. T-cadherin supports angiogenesis and adiponectin association with the vasculature in a mouse mammary tumor model. *Cancer Res*. 2008;68(5):1407–1416.
30. Maeda N, et al. Diet-induced insulin resistance in mice lacking adiponectin/ACRP30. *Nat Med*. 2002;8(7):731–737.
31. Shibata R, et al. Adiponectin-mediated modulation of hypertrophic signals in the heart. *Nat Med*. 2004;10(12):1384–1389.
32. Li J, et al. Cardiac-specific loss of N-cadherin leads to alteration in connexins with conduction slowing and arrhythmogenesis. *Circ Res*. 2005;97(5):474–481.
33. Zuppinger C, Eppenberger-Eberhardt M, Eppenberger HM. N-Cadherin: structure, function and importance in the formation of new intercalated disc-like cell contacts in cardiomyocytes. *Heart Fail Rev*. 2000;5(3):251–257.
34. Zhang P, et al. AMP activated protein kinase-alpha2 deficiency exacerbates pressure-overload-induced left ventricular hypertrophy and dysfunction in mice. *Hypertension*. 2008;52(5):918–924.
35. Sano M, et al. p53-induced inhibition of Hif-1 causes cardiac dysfunction during pressure overload. *Nature*. 2007;446(7134):444–448.
36. Shimano M, et al. Adiponectin deficiency exacerbates cardiac dysfunction following pressure overload through disruption of an AMPK-dependent angiogenic response. *J Mol Cell Cardiol*. 2010; 49(2):210–220.
37. Denzel MS, Hebbard LW, Shostak G, Shapiro L, Cardiff RD, Ranscht B. Adiponectin deficiency limits tumor vascularization in the MMTV-PyV-mT mouse model of mammary cancer. *Clin Cancer Res*. 2009;15(10):3256–3264.
38. Landskroner-Eiger S, et al. Proangiogenic contribution of adiponectin toward mammary tumor growth in vivo. *Clin Cancer Res*. 2009;15(10):3265–3276.
39. Shibata R, et al. Adiponectin protects against the development of systolic dysfunction following myocardial infarction. *J Mol Cell Cardiol*. 2007; 42(6):1065–1074.
40. Shibata R, et al. Adiponectin protects against myocardial ischemia-reperfusion injury through AMPK- and COX-2-dependent mechanisms. *Nat Med*. 2005;11(10):1096–1103.
41. Meerson FZ. On the mechanism of compensatory hyperfunction and insufficiency of the heart. *Cor Vasa*. 1961;3:161–177.
42. Shibata R, Ouchi N, Kihara S, Sato K, Funahashi T, Walsh K. Adiponectin stimulates angiogenesis in response to tissue ischemia through stimulation of amp-activated protein kinase signaling. *J Biol Chem*. 2004;279(27):28670–28674.
43. Maron BJ, Roberts WC, McAllister HA, Rosing DR, Epstein SE. Sudden death in young athletes. *Circulation*. 1980;62(2):218–229.
44. Semsarian C, et al. The L-type calcium channel inhibitor diltiazem prevents cardiomyopathy in a mouse model. *J Clin Invest*. 2002;109(8):1013–1020.
45. Frystyk J, Berne C, Berglund L, Jensevik K, Flyvbjerg A, Zethelius B. Serum adiponectin is a predictor of coronary heart disease: a population-based 10-year follow-up study in elderly men. *J Clin Endocrinol Metab*. 2007;92(2):571–576.
46. Pischon T, Girman CJ, Hotamisligil GS, Rifai N, Hu FB, Rimm EB. Plasma adiponectin levels and risk of myocardial infarction in men. *JAMA*. 2004; 291(14):1730–1737.
47. Mukoyama Y, Utani A, Matsui S, Zhou S, Miyachi Y, Matsuyoshi N. T-cadherin enhances cell-matrix adhesiveness by regulating beta1 integrin trafficking in cutaneous squamous carcinoma cells. *Genes Cells*. 2007;12(6):787–796.
48. Joshi MB, Ivanov D, Philippova M, Erne P, Resink TJ. Integrin-linked kinase is an essential mediator for T-cadherin-dependent signaling via Akt and GSK3beta in endothelial cells. *FASEB J*. 2007; 21(12):3083–3095.
49. Dallabrida SM, et al. Integrin binding angiopoietin-1 monomers reduce cardiac hypertrophy. *FASEB J*. 2008;22(8):3010–3023.
50. Fujioka D, et al. Role of adiponectin receptors in endothelin-induced cellular hypertrophy in cultured cardiomyocytes and their expression in infarcted heart. *Am J Physiol Heart Circ Physiol*. 2006; 290(6):H2409–H2416.
51. Lee MH, Klein RL, El-Shewy HM, Luttrell DK, Luttrell LM. The adiponectin receptors AdipoR1 and AdipoR2 activate ERK1/2 through a Src/Ras-dependent pathway and stimulate cell growth. *Biochemistry*. 2008;47(44):11682–11692.
52. Jee SH, et al. Adiponectin concentrations: a genome-wide association study. *Am J Hum Genet*. 2010; 87(4):545–552 .